Δ9-Tetrahydrocannabinol-Induced Apoptosis in Jurkat Leukemia T Cells Is Regulated by Translocation of Bad to Mitochondria

Wentao Jia,[2] Venkatesh L. Hegde,[1] Narendra P. Singh,[1] Daniel Sisco,[1] Steven Grant,[3] Mitzi Nagarkatti,[1] and Prakash S. Nagarkatti[1]

[1]Department of Pathology, Microbiology, and Immunology, University of South Carolina School of Medicine, Columbia, South Carolina and Departments of [2]Pharmacology and Toxicology and [3]Medicine, Medical College of Virginia Campus, Virginia Commonwealth University, Richmond, Virginia

Abstract

Plant-derived cannabinoids, including Δ9-tetrahydrocannabinol (THC), induce apoptosis in leukemic cells, although the precise mechanism remains unclear. In the current study, we investigated the effect of THC on the upstream and downstream events that modulate the extracellular signal-regulated kinase (ERK) module of mitogen-activated protein kinase pathways primarily in human Jurkat leukemia T cells. The data showed that THC down-regulated Raf-1/mitogen-activated protein kinase/ERK kinase (MEK)/ERK/RSK pathway leading to translocation of Bad to mitochondria. THC also decreased the phosphorylation of Akt. However, no significant association of Bad translocation with phosphatidylinositol 3-kinase/Akt and protein kinase A signaling pathways was noted when treated cells were examined in relation to phosphorylation status of Bad by Western blot and localization of Bad to mitochondria by confocal analysis. Furthermore, THC treatment decreased the Bad phosphorylation at Ser[112] but failed to alter the level of phospho-Bad on site Ser[136] that has been reported to be associated with phosphatidylinositol 3-kinase/Akt signal pathway. Jurkat cells expressing a constitutively active MEK construct were found to be resistant to THC-mediated apoptosis and failed to exhibit decreased phospho-Bad on Ser[112] as well as Bad translocation to mitochondria. Finally, use of Bad small interfering RNA reduced the expression of Bad in Jurkat cells leading to increased resistance to THC-mediated apoptosis. Together, these data suggested that Raf-1/MEK/ERK/RSK-mediated Bad translocation played a critical role in THC-induced apoptosis in Jurkat cells. (Mol Cancer Res 2006;4(8):549–62)

Copyright © 2006 American Association for Cancer Research.
doi:10.1158/1541-7786.MCR-05-0193

Introduction

Cannabinoids, the biologically active constituents of marijuana (*Cannabis sativa*), produce a wide spectrum of central and peripheral effects, such as alterations in cognition and memory, analgesia, anticonvulsion, anti-inflammation, and alleviation of both intraocular pressure and pain relief (1). There has been a growing interest in cannabinoids since the cloning of two subtypes of the cannabinoid receptors, CB1 (2) and CB2 (3). The CB1 receptor is mainly expressed in the central nervous system, whereas the CB2 receptor is predominantly expressed in immune cells (4). Both cannabinoid receptors are coupled to heterotrimeric $G_{i/o}$ proteins and interact with the mitogen-activated protein kinases (MAPK), particularly the extracellular signal-regulated kinase (ERK; ref. 5).

At almost the same time, endogenous ligands for these receptors, capable of mimicking, to some extent, the pharmacologic actions of marijuana's psychoactive principle Δ9-tetrahydrocannabinol (THC), have been discovered (6). Numerous studies have shown that THC can modulate the functions of immune cells (7). More recently, we reported that the immunosuppressive property of THC can be attributed, at least in part, to its ability to induce apoptosis in T cells and dendritic cells through ligation of CB2 receptors and that the latter was regulated by activation of nuclear factor-κB (8), recruiting both intrinsic and extrinsic pathways of apoptosis. Interestingly, we also found that THC and other cannabinoids could induce apoptosis in transformed murine and human T cells (9), including primary acute lymphoblastic human leukemia cells, and furthermore that the treatment of mice bearing a T-cell leukemia with THC could cure ∼25% of the mice (10). These findings are consistent with studies showing that THC and other cannabinoids can induce apoptosis in a variety of tumor cell lines, thereby raising the possibility of the use of cannabinoids as novel anticancer agents (11).

The precise mechanism through which cannabinoids induce apoptosis is under active investigation and may vary based on cell type. In normal and transfected neural cells, vascular endothelial cells, and Chinese hamster ovary cells, cannabinoid treatment was shown to induce activation of ERK (12), c-Jun NH₂-terminal kinase (JNK), and p38 (13, 14). In contrast, it was shown that cannabinoids were cytotoxic in leukemic cells and that they inhibited neuronal progenitor cell differentiation through attenuation of the ERK pathway (15). In glioma cells, THC was shown to induce apoptosis via ceramide generation

(16). However, cannabinoids can also block ceramide-induced apoptosis of normal astrocytes (17). Together, such studies suggest that the precise signaling pathways that are evoked by cannabinoid receptor activation in normal and transformed cells may vary based on cell type and that such activation could lead to the generation of survival or death signals.

In the current study, we investigated the molecular mechanisms underlying apoptosis induced by THC, specifically addressing the role of MAPK signaling. Treatment with THC caused interruption of the MAPK/ERK kinase (MEK)/ERK signaling module that was required for apoptotic lethality, and this event possibly played an important functional role in mediating THC-induced translocation of Bad to mitochondria.

Results

Treatment of Jurkat Cells with THC Induces Suppression of the Raf-1/MEK/ERK Cytoprotective Signaling Pathway through the Signaling of the Cannabinoid Receptors

To gain insights into the functional role of cannabinoid receptor pathway in THC-mediated lethality, Jurkat cells were pretreated with either SR141716 (CB1 antagonist) or SR144528 (CB2 antagonist) in the absence or presence of THC for a designated period (6-30 hours), after which the percentage of cells displaying the morphologic features of apoptosis was determined by the Wright-Giemsa-stained cytospin preparation. THC caused dose-dependent apoptosis in Jurkat cells (data not shown) with a very substantial increase in cell death detected at 10 μmol/L (Fig. 1A). Time course analysis revealed that exposure to SR141716 (CB1 antagonist) or SR144528 (CB2 antagonist) individually at the concentration of 1 or 2 μmol/L were minimally toxic over 30-hour treatment interval, whereas treatment with 10 μmol/L THC alone caused ∼50% apoptosis (Fig. 1A). However, when cells were pretreated with either SR141716 or SR144528 followed by exposure to THC, there was a significant reduction in apoptosis by 6 hours and a very substantial reversal in lethality after 12 hours (Fig. 1A). Very similar results were obtained when THC-treated cells were evaluated for combined early and late apoptotic cells by Annexin V/propidium iodide (PI) analysis (Fig. 1B). In this assay, cells stained for Annexin V alone are considered to be early apoptotic cells and those stained for Annexin V and PI represent late apoptotic cells. We also analyzed the cells for loss of mitochondrial membrane potential (MMP; $\Delta\psi_m$) as described (10) and designated them as cells with ''low'' 3,3-dihexyloxacarbocyanine iodide uptake (Fig. 1B). Next, we measured the levels of CB1 and CB2 receptors in Jurkat cells and compared them with other tumor cell lines, such as the T-cell lymphoma Hut78 and the glioma U251 known to express CB1 receptors. As shown in Fig. 1C, Jurkat and Hut78 but not U251 cells expressed significant levels of CB2 mRNA. In addition, when CB1 mRNA levels were analyzed, Jurkat cells were found to express low levels. Interestingly, when all cells were cultured with THC, CB1 and CB2 receptor expression was significantly increased. These data explained why in Jurkat cells not only CB2 antagonist but also CB1 antagonist were able to partially block THC-induced apoptosis.

To further characterize the downstream signaling pathways that trigger apoptosis following activation of cannabinoid receptors, Jurkat cells were pretreated with either CB1 or CB2 antagonists in the absence or presence of THC for 12 hours. As shown in Fig. 1D, THC treatment of Jurkat cells caused reduced phosphorylation of Raf-1, whereas total protein levels remained constant. In addition, exposure of cells to THC diminished the levels of phosphorylation of MEK1/2, with the total MEK1/2 expression remaining unchanged. Similarly, phosphorylation of ERK1/2 was largely decreased in THC-treated cells, but total ERK1/2 expression remained unperturbed. In contrast, when cells were pretreated with CB1 or CB2 antagonists, the effects of THC on each of these proteins were largely reduced. None of the THC concentrations tested induced alterations in phospho-p38 or phospho-JNK. In addition, no changes were observed in levels of total p38 or JNK. Consequently, we evaluated the levels of phospho-p90RSK (Thr[359]/Ser[363]), phospho-p90RSK (Ser[380]), phospho-p90RSK (Thr[573]), and total p90RSK following exposure of Jurkat cells to THC in the absence or presence of CB1/2 antagonists (Fig. 1D). THC caused a reduction in p90RSK phosphorylation involving both Thr[359]- and Ser[363]-specific phosphorylation sites. However, when cells were pretreated with CB1 or CB2 antagonist, the effects of THC on both phosphorylation sites of this protein were significantly reversed. No changes were detected in levels of total p90RSK or phospho-p90RSK on sites Ser[380] and Thr[573]. Attempts also were made to extend ERK inactivation to other human tumor cell lines. As shown in Fig. 1E, an 18-hour exposure of Molt4, Hut78, and SupT1 cells to THC resulted in a marked reduction in the levels of phospho-ERK1/2, with the total ERK1/2 expression remaining unchanged. Finally, essentially similar results were obtained when the effects of THC were examined in kinase activity. A decrease in ERK activity was detectable in Jurkat cells after treatment with THC beginning at hour 1, and this effect was even more pronounced at 12 hours (Fig. 1F). Taken together, these data suggest that suppression of the Raf-1/MEK/ERK cytoprotective signaling pathway by THC may play an important functional role in the induction of apoptosis in Jurkat cells as well as in other tumor cell lines tested.

Caspase-Independent Events in Raf-1/MEK/ERK Signaling

To determine the role caspase activation in THC-mediated perturbations in ERK signaling, Jurkat cells were pretreated with pan-caspase inhibitor Z-VAD-FMK in the presence or absence of THC. As shown in Fig. 2A, caspase inhibition failed to alter the THC-mediated down-regulation of phosphorylation of Raf-1, MEK1/2, ERK1/2, and RSK (Thr[359]/Ser[363]). No changes were noted in the levels of total Raf-1, MEK1/2, ERK1/2, and RSK or phospho-p90RSK on sites Ser[380] and Thr[573]. These results indicated that in Jurkat cells down-regulation of the Raf-1/MEK/ERK/RSK axis represents an early consequence of the treatment of cells with THC and that it proceeds in a caspase-independent manner. As shown in Fig. 2B, exposure of Jurkat cells to Z-VAD-FMK significantly inhibited THC-induced procaspase-10, procaspase-2, procaspase-8, procaspase-9, procaspase-3, and Bid processing as well as poly(ADP-ribose) polymerase (PARP) degradation. It should
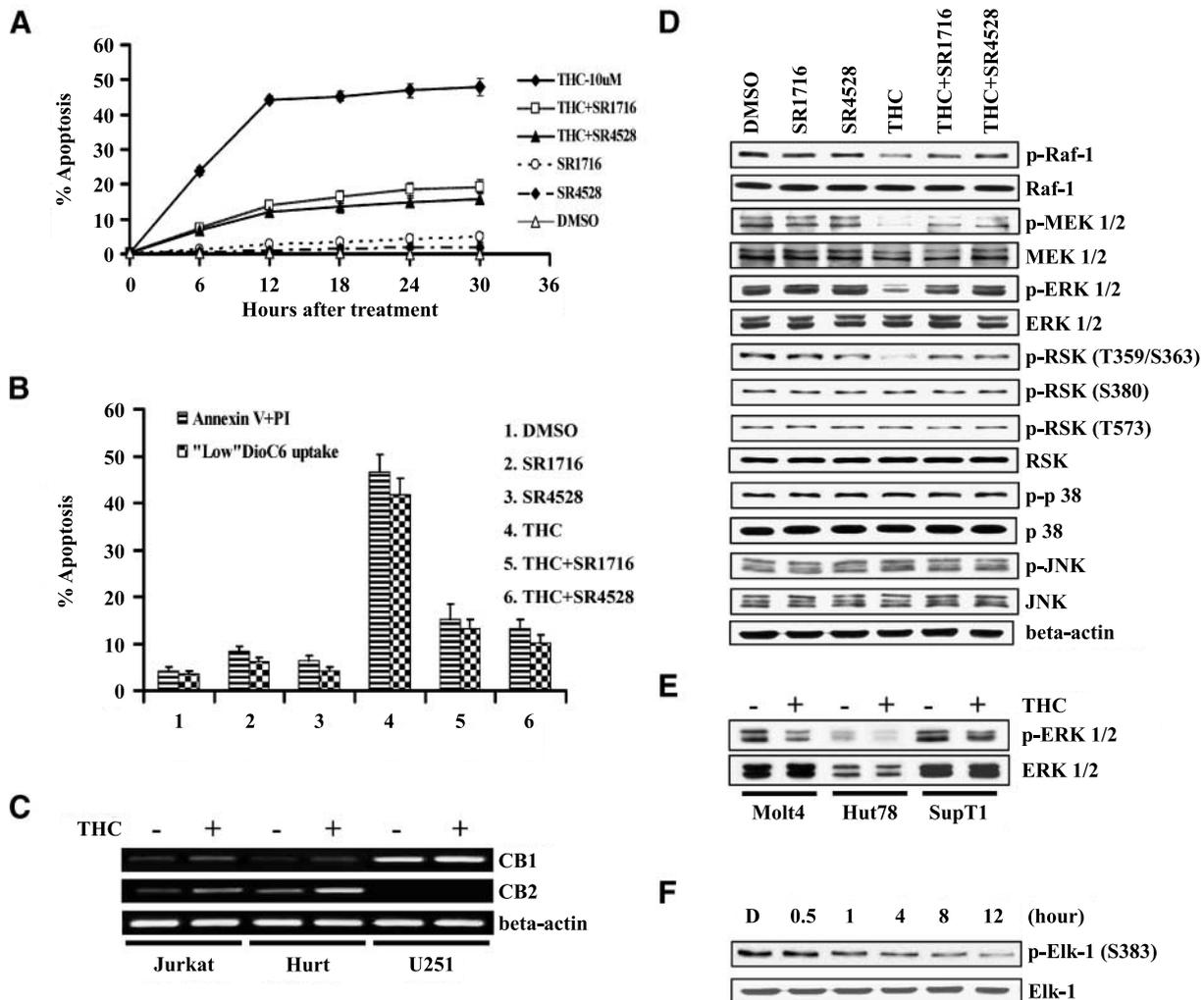
FIGURE 1. Effects of THC on Raf-1/MEK/ERK signaling in Jurkat cells. **A.** Jurkat cells were pretreated with either 1 μmol/L SR141716 or 2 μmol/L SR144528 in medium containing 10% FBS in the absence or presence of 10 μmol/L THC for a designated period (6-30 hours), after which the percentage of apoptosis was determined by examining Wright-Giemsa-stained cytospin preparations as described in Materials and Methods. Points, mean percent apoptosis of at least three separate experiments done in triplicate; bars, SD. **B.** Cells were treated as described in **A** for 12 hours, after which the extent of apoptosis and loss of MMP were monitored by Annexin V/PI staining and 3,3-dihexyloxacarbocyanine iodide uptake, respectively. Columns, mean percent apoptosis of three separate experiments done in triplicate; bars, SD. **C.** Expression of CB1 and CB2 was determined by reverse transcription-PCR analysis. Total RNA was isolated from Jurkat, Hut78, and U251 tumor cells, which were either left untreated or treated with THC. mRNA was reverse transcribed and amplified by PCR with primers specific for CB1 and CB2. Photograph of ethidium bromide–stained amplicons. **D.** Cells were treated as described in **A** for 12 hours, after which the Western analysis was used to monitor expression of phospho-Raf-1, Raf-1, phospho-MEK1/2, MEK1/2, phospho-ERK1/2, ERK1/2, phospho-RSK (Thr^{359}/Ser^{363}), phospho-RSK (Ser^{380}), phospho-RSK (Thr^{573}), RSK, phospho-p38, p38, phospho-JNK, and JNK. β-Actin served as loading control. **E.** Molt4, Hut78, and SupT1 cells were either left untreated or treated with THC at designated concentrations (7.5, 5, and 10 μmol/L, respectively) in medium containing 10% FBS for 18 hours, after which the levels of phosphor-ERK1/2 and total ERK1/2 were monitored by Western blot. ERK1/2 served as loading control. **F.** Jurkat cells were either left untreated or treated with 10 μmol/L THC for a designated interval (from 0.5 to 12 hours), after which an ERK kinase assay was done by immunoprecipitation of ERK using a monoclonal phospho-ERK1/2 (Thr^{202}/Tyr^{204}). The immunoprecipitate was subsequently incubated with an Elk-1 fusion protein in the presence of ATP, which allowed precipitated phospho-ERK to phosphorylate Elk-1, a major substrate of phospho-ERK. D, DMSO. Elk-1 served as loading controls. Representative of a minimum of three separate experiments.

be noted that treatment of Jurkat cells with Z-VAD-FMK alone did not alter the expression of any of the molecules under investigation (data not shown).

Antiapoptotic Effect of Phorbol 12-Myristate 13-Acetate Depends on ERK Activation

To confirm the possible role of ERK activation in THC-induced apoptosis, Jurkat cells were pretreated with 10 nmol/L phorbol 12-myristate 13-acetate (PMA), a potent activator of ERK (18, 19). Next, the cells were treated with 10 μmol/L THC for a total of 12 hours or left untreated. Parallel studies were done on cells precultured with 25 μmol/L U0126, a MEK inhibitor. The extent of apoptosis was then determined by terminal deoxynucleotidyl transferase–mediated dUTP end labeling (TUNEL) assay. Treatment of cells with THC alone for 12 hours caused ~43% apoptosis, which was partially

blocked in the presence of either CB1 or CB2 antagonist, thereby confirming the involvement of CB1 and CB2 receptors in apoptosis (Fig. 3A). In addition, THC-induced apoptosis was also partially blocked by PMA (Fig. 3A). Moreover, treatment of cells with U0126 alone caused significant levels of apoptosis consistent with our hypothesis that MEK inhibition in Jurkat cells can lead to cell death. Furthermore, the combination of THC plus U0126 caused a marked increase in apoptosis, which was more than that seen when either of these compounds was used alone. As expected, treatment with PMA plus U0126 caused a significant inhibition in apoptosis when compared with the use of U0126 alone. To characterize interaction between THC and U0126 more rigorously and over a range of drug concentrations at a fixed ratio (1:2.5), median dose effect analysis was used. When the extent of apoptosis was determined, combination index values considerably less than 1.0 were obtained (Fig. 3B), corresponding to highly synergistic interaction. These data together suggest that THC-induced ERK inactivation may play a critical role in apoptosis in Jurkat cells.

Next, we determined protein levels of phospho-ERK to see what protective action was mediated by PMA in THC-treated cells. As shown in Fig. 3C, incubation with PMA alone induced increased phosphorylation of ERK1/2. When cells were exposed to PMA followed by THC, there was significant reversal in phospho-ERK1/2 levels. In contrast, treatment with U0126 alone caused a significant decrease in phospho-ERK1/2, whereas the combination of U0126 plus THC resulted in essentially the complete disappearance of phospho-ERK1/2. PMA was a potent activator of ERK as has also been reported by others (18, 19), inasmuch as it reversed the effect of the combined treatment of U0126 plus THC on ERK1/2. These data were corroborated determining the levels of the phosphorylation

of ERK1/2 by densitometric analysis (Fig. 3D). Finally, the effect of these agents, alone and in combination, were examined in relation to caspase cascades in THC-treated cells (Fig. 3E). Whereas U0126 alone had a demonstrable effect on the activation of all caspases tested as well as on the cleavage of caspases and PARP, treatment with THC alone caused much more cleavage of each of these proteins, consistent with the increased levels of apoptosis observed previously. Treatment with PMA blocked the THC-induced activation of caspases and other markers of apoptosis. Caspase analysis using U0126 alone, PMA plus U0126, and U0126 plus THC was all consistent with the above observation on the ability of U0126 to enhance and PMA to block apoptosis in THC-treated Jurkat cells.

Enforced Activation of MEK1/ERK Substantially Blocks THC-Mediated Caspase Activation, DNA Fragmentation, and Apoptosis

To further define the functional role of MEK/ERK, a Jurkat cell line that inducibly expresses a constitutively active MEK1 construct (Mek/30) under the control of a doxycycline-responsive promoter was employed. As shown in Fig. 4A, exposure to THC in the absence of doxycycline resulted in apoptosis in ~50% of cells, whereas apoptosis was markedly reduced in the presence of doxycycline at 12 hours ($P < 0.05$), and these effects were even more pronounced at 24 hours ($P < 0.005$; data not shown). Similar results were obtained with a second MEK1-inducible clone (Jurkat Mek/6; data not shown). Western analysis revealed that cells cultured in the absence of doxycycline displayed minimal expression of a hemagglutinin tag and modest basal expression of phospho-MEK (Fig. 4B). However, when cells were cultured in the presence of doxycycline, a pronounced increase in expression of the hemagglutinin tag was noted along with substantial increases in expression of phospho-MEK, phospho-ERK, and phospho-RSK (Thr^{359}/Ser^{363}). Enforced activation of MEK also diminished THC-mediated activation of procaspase-8, procaspase-9, procaspase-3, and Bid processing as well as PARP degradation. Analogous to results obtained with the inducible MEK system, in the absence of doxycycline, THC treatment alone resulted in the induction of DNA fragmentation (Fig. 4C). When cells were cultured in the presence of doxycycline, DNA degradation was significantly blocked. Together, these data suggest that Raf-1/MEK/ERK/RSK pathways play an important functional role in THC-induced apoptosis.

Pertussis Toxin Pretreatment Prevents THC-Induced Cell Death

Next, we examined the relationship between receptor-mediated activation of the G protein and THC-mediated apoptosis. To this end, Jurkat cells were exposed to either 50 or 100 ng/mL pertussis toxin (PTX) for 16 hours in the absence or presence of 10 μmol/L THC for an additional 12 hours. As shown in Fig. 5A, pretreatment with PTX caused a significant inhibition in THC-induced apoptosis. In related studies, the effect of PTX was also monitored with respect to MAPK signaling and the activation of apoptotic regulatory proteins induced by THC. Exposure of cells to PTX reversed the THC-mediated reduction in expression of phospho-Raf-1 as well as phosphorylation of MEK1/2, ERK1/2, and RSK
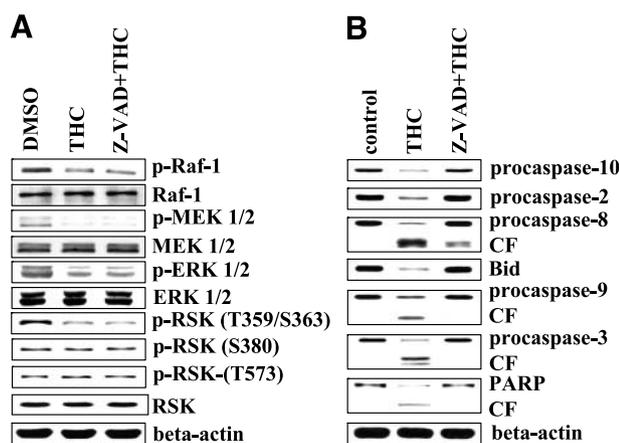
FIGURE 2. Effect of exposure of Jurkat cells to pan-caspase inhibitor, Z-VAD-FMK. Jurkat cells were pretreated with 20 μmol/L Z-VAD-FMK in medium containing 10% FBS in the presence or absence of 10 μmol/L THC for a total 12 hours, after which Western analysis was done to monitor expression of (**A**) phospho-Raf-1, Raf-1, phospho-MEK1/2, MEK1/2, phospho-ERK1/2, ERK1/2, phospho-RSK (Thr[359]/Ser[363]), phospho-RSK (Ser[380]), phospho-RSK (Thr[573]), and RSK and after 24 hours to monitor expression of (**B**) procaspase-10, procaspase-2, procaspase-8, Bid, procaspase-9, procaspase-3, and PARP or cleaved fragments (*CF*). β-Actin served as a loading control. Representative experiment. Two additional studies yielded similar results.
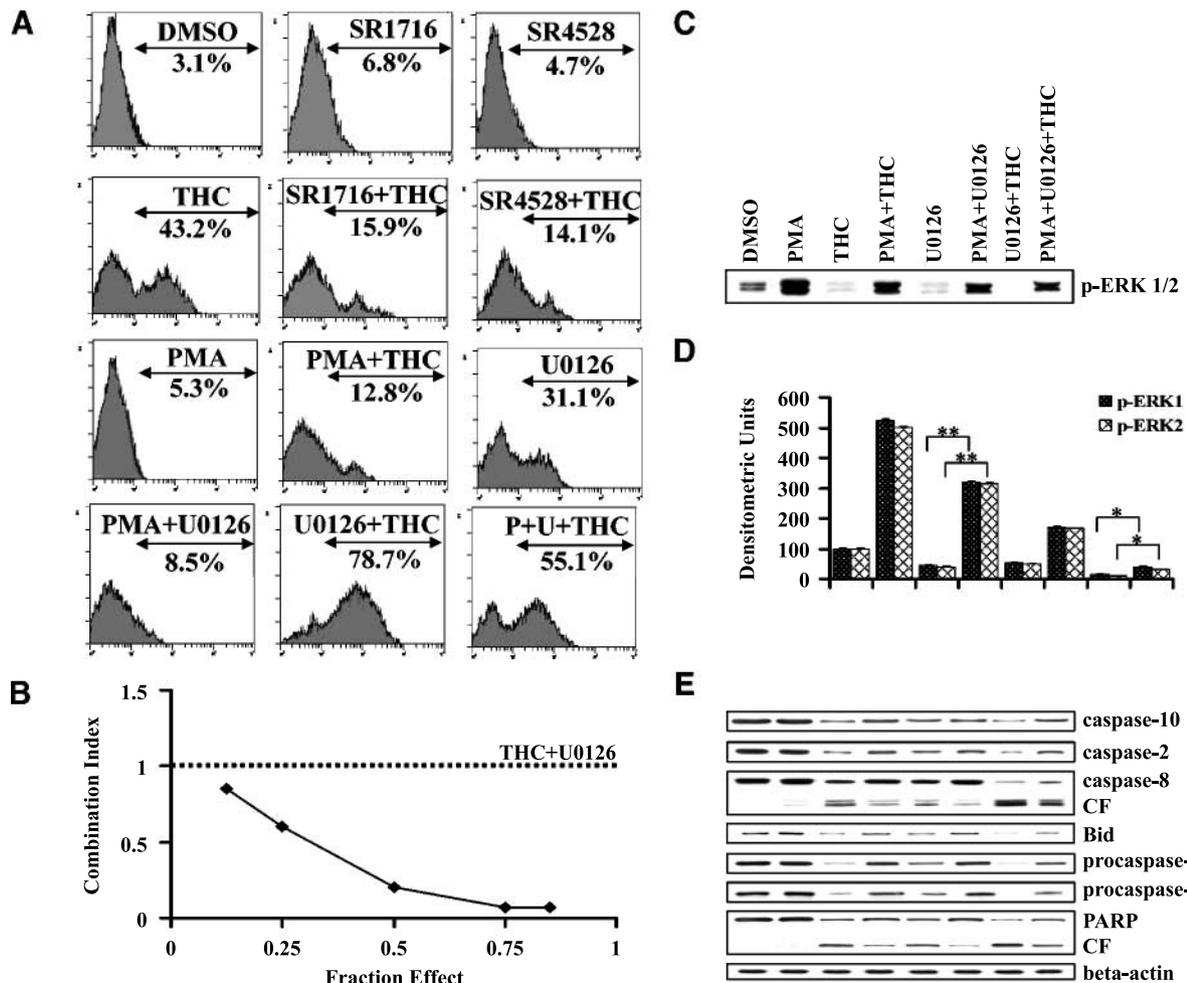
FIGURE 3. Role of ERK action in the regulation of THC-induced apoptosis. **A.** Jurkat cells were first cultured to 1 μmol/L SR141716, 2 μmol/L SR144528, 10 nmol/L PMA, or 25 μmol/L U0126 in medium containing 10% FBS in the absence or presence of 10 μmol/L THC for a total 12 hours, after which the extent of apoptosis was analyzed by TUNEL assay. TUNEL-positive cells were quantified by flow cytometric analysis. **B.** Jurkat cells were exposed to varying concentration of THC and U0126 at a fixed ratio (1:2.5) for 24 hours, after which the percentage of apoptosis was determined as described in Fig. 1A. Median dose effect analysis was used to determine the combination index for each fraction effect. Combination indices < 1.0 correspond to synergistic interactions. Representative experiment; three independent experiments done in triplicate. **C.** Lysates prepared from cells pretreated with 10 nmol/L PMA or 25 μmol/L U0126 in medium containing 10% FBS in the absence or presence of 10 μmol/L THC for 12 hours were blotted and probed for phospho-ERK1/2. Representative experiment. Two additional studies yielded similar results. **D.** Quantitative changes in ERK1/2 phosphorylation were determined by densitometric analysis of immunoblots. Columns, mean of triplicate determinations in five separate experiments; bars, SD. *, $P < 0.05$, **, $P < 0.005$. **E.** Samples collected from cells cultured as described in **C** for 24 hours in medium containing 10% FBS were monitored for protein levels of procaspase-10, procaspase-2, procaspase-8, Bid, procaspase-9, procaspase-3, PARP, and cleaved fragments. Representative of a minimum of three separate experiments.

(Thr^{359}/Ser^{363}; Fig. 5B). Similarly, PTX treatment reversed other THC-mediated effects, including cleavage of procaspase-10, procaspase-2, procaspase-8, procaspase-9, procaspase-3, and Bid and degradation of PARP (Fig. 5B). Together, these data suggest a role for G-protein signaling in THC-induced MAPK signaling, caspase activation, and apoptosis.

THC Down-Regulates the Raf-1/MEK/ERK/RSK Signaling Pathway and Triggers Mitochondrial Localization of Bad

Recently, the MAPK-activated RSK was shown to promote cell survival through phosphorylation and inactivation of the proapoptotic Bcl-2 family member, Bad (18). In addition, mitochondrial membrane-based protein kinase A (PKA) and Akt, a kinase activated by growth factors through a phospha-

tidylinositol 3-kinase (PI3K)–dependent mechanism, could also be implicated in Bad phosphorylation. To this end, we examined whether Bad played a role in THC-induced apoptosis involving Akt and PKA signaling pathways. First, Jurkat cells were cultured with either 15 μmol/L LY294002, a PI3K inhibitor, or 2 μmol/L H-89, a PKA inhibitor. Next, the cells were treated with 10 μmol/L THC for a total of 12 hours or left untreated. The percentage of apoptotic cells was then determined by examining Wright-Giemsa-stained cytospin preparations. As shown in Fig. 6A, coadministration of LY294002 at a concentrations of 15 μmol/L, which was minimally toxic alone, resulted in apoptosis in majority of THC-treated cells. A very similar pattern was noted when the extent of apoptosis was determined by TUNEL assay (data not
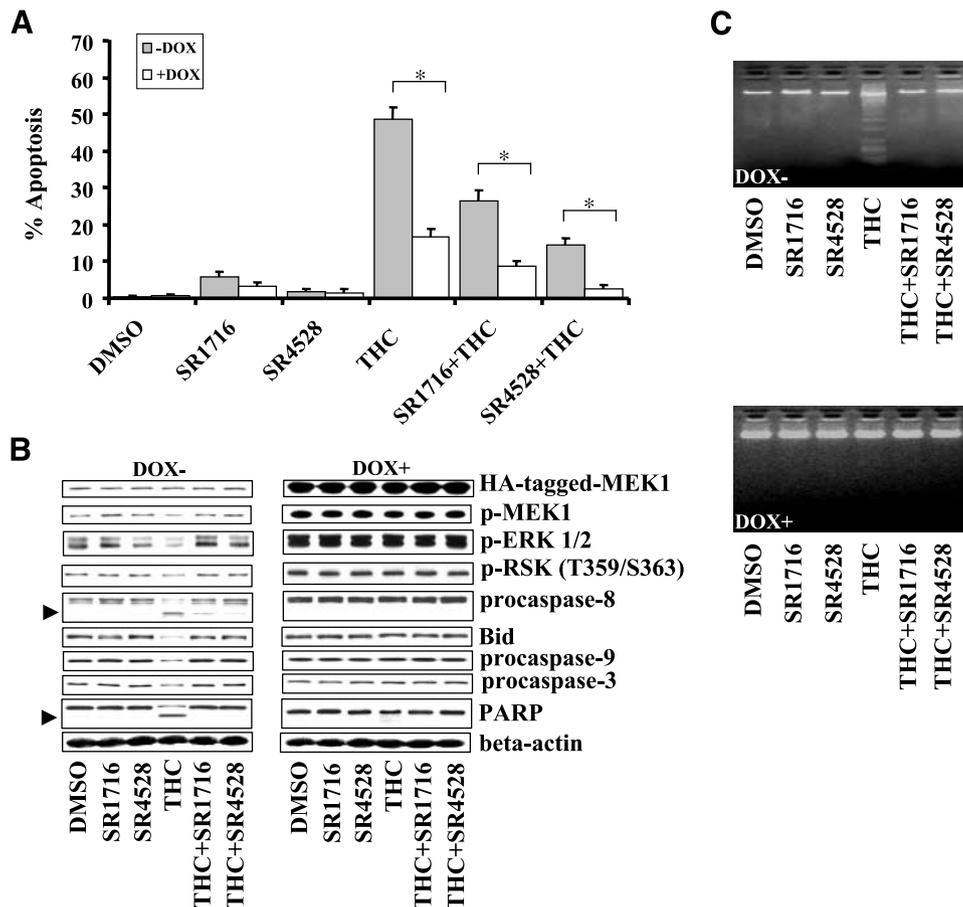
FIGURE 4. Enforced activation of MEK/ERK blocks THC-mediated apoptosis. A. Jurkat cells inducibly expressing a constitutively active, hemagglutinin-tagged MEK1 vector under the control of a tetracycline-responsive promoter were exposed to either 1 μmol/L SR141716 or 2 μmol/L SR144528 followed by 10 μmol/L THC for 12 hours in the presence or absence of 2 μg/mL doxycycline (DOX). Percentage of apoptotic cells was then determined as described in Fig. 1A. Columns, mean of three separate experiments; bars, SD. *, $P < 0.05$, significantly less than values obtained for the treated cells in the absence of doxycycline. B. Cells were treated as described in A. Proteins (prepared from cells in the absence and presence of doxycycline) were transferred onto a single piece of nitrocellulose following fractionation using the same gel, and Western analysis was used to monitor expression of the hemagglutinin (HA)–tagged MEK, phospho-MEK, phospho-ERK, and phospho-RSK (Thr[359]/Ser[363]) at exactly same incubation time. Levels of caspases and PARP were immunoassayed by culturing Jurkat cells for 24 hours as described in A. Arrows, THC-induced breakdown products or active caspases. β-Actin served as a loading control. Representative experiment. An additional study yielded equivalent results. C. Cells were treated for 24 hours as described in A, after which DNA was isolated and subjected to agarose gel electrophoresis. Gels were stained with ethidium bromide and viewed under UV light.
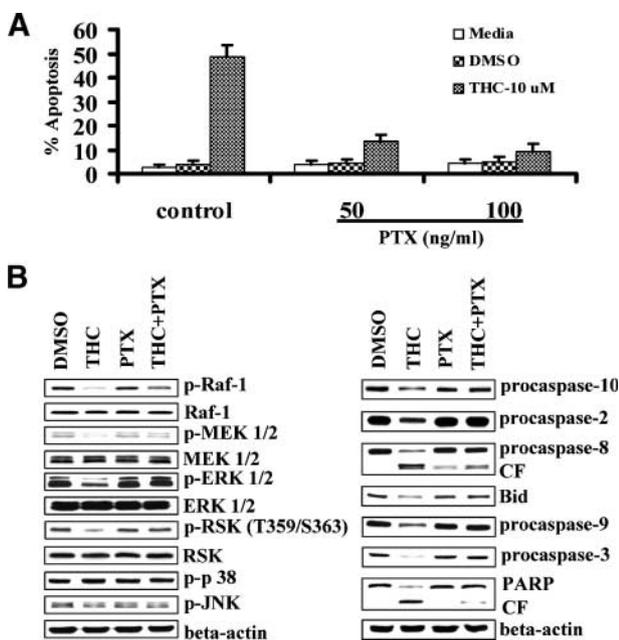
shown). However, no involvement of the PKA event was noted when cells were exposed to THC in combination with H-89 (Fig. 6A). Western blot analysis (Fig. 6B) revealed that combined treatment with THC and LY294002 (12 hours) resulted in a down-regulation in Akt phosphorylation involving both Thr[308]- and Ser[473]-specific phosphorylation sites, which was more than that seen when either of these compounds was used alone. No changes were observed in the levels of total Akt with any treatments.

To examine whether the Akt pathway suppressed by THC may play a role in dephosphorylation of Bad with the cell death, Jurkat cells were stimulated with either LY294002 or U0126 at designated concentrations. Subsequently, the cells were treated with 10 μmol/L THC for a total 12 hours or left untreated. The phosphorylation status of Bad was monitored by the immuno-precipitation following by Western analyses. As shown in Fig. 6C, THC and U0126 alone diminished the levels of phosphorylation of Bad on site Ser[112], whereas the levels of

phospho-Bad on site Ser[136] remained unchanged. When cells were exposed to THC in combination with U0126, there was a significant reduction and essentially the complete disappear-ance of phospho-Bad (Ser[112]) levels. In contrast, coadminista-tion of THC plus LY294002 did not enhance the degree of the dephosphorylation of Bad on site Ser[136] when this was compared with LY294002 treatment alone. Furthermore, treatment of Jurkat cells with THC alone at the concentration (5-15 μmol/L) of THC and the time course analyses (30 minutes to 30 hours) did not alter the level of phospho-Bad on site Ser[136] under investigation (only one data point shown). No significant changes were observed in the levels of phospho-Bad on site Ser[155] with any treatments (Fig. 6C). These results were confirmed using densitometric analysis (Fig. 6D), which distinguishes the changes of Bad phosphor-ylation after designated treatment.

Lastly, the effects of combined exposure to THC were examined in relation to the localization of Bad. Generally, Bad

resides in the cytosol but translocates to the mitochondria following death signaling. We therefore used confocal microscopy to study the translocation of Bad following exposure of Jurkat cells to THC alone or in combinations with other treatments. Double-immunofluorescence analysis with anti-Bad antibody and mitochondria-specific dye (MitoTracker Deep Red 633) showed a strong association of Bad with mitochondria in THC-treated cells compared with vehicle-treated cells (Fig. 6E). To further establish a link between the MEK/ERK pathway and the translocation of Bad to the mitochondria in THC-treated Jurkat cells, we used U0126, a potent inhibitor of this pathway. In addition, we used LY294002 to see whether combined treatment with LY294002 and THC could enhance the translocation of Bad to the mitochondria. The data shown in Fig. 6E indicated that exposure to U0126 significantly enhanced THC-induced translocation of Bad to the mitochondria and that a combination of THC plus U0126 caused marked increase in Bad translocation to mitochondria. In addition, treatment of Jurkat cells with LY294002 alone induced minimal Bad translocation and THC plus LY294002 did not augment this process when compared with THC alone (Fig. 6E). These findings together suggested that THC induced the translocation of Bad to mitochondria without significant association of Bad with PI3K/Akt pathway.

To further determine whether THC induced translocation of Bad via the interruption of Raf-1/MEK/ERK/RSK pathway, Jurkat cells were stably transfected with a constitutively active MEK1 construct (Mek/30). As shown in Fig. 7A, exposure to either THC or U0126 in the absence of doxycycline resulted in dephosphorylation of Bad on site Ser^{112}, and these effects were even more pronounced when cells were treated with THC plus U0126. Similar results were obtained with a second MEK1-inducible clone (Jurkat Mek/6; data not shown). However, when cells were cultured in the presence of doxycycline, THC-induced down-regulation of Bad on this site was blocked. No changes were detected in levels of phosphorylation of Bad on other sites when cells were cultured in the absence or presence of doxycycline. Confocal analysis revealed that cells cultured in the absence of doxycycline displayed a strong association of Bad with mitochondria in THC plus U0126–treated cells, which was more than that seen when either of these compounds was used alone (Fig. 7B). However, when cells were cultured in the presence of doxycycline, enforced activation of MEK/ERK/RSK significantly blocked THC-mediated translocation of Bad to the mitochondria, analogous to results obtained with a second MEK1-inducible clone (Jurkat Mek/6; data not shown). Together, these findings suggest that suppression of Raf-1/MEK/ERK/RSK signaling pathway by THC plays an important functional role in the induction of Bad translocation to the mitochondria.

To confirm the requirement of Bad in THC-induced apoptosis of Jurkat cells, we used a RNA interference approach. It has been shown that small interfering RNA (siRNA) consisting of 21-bp dsRNA can mediate RNA interference effect in mammalian cells. We used two types of Bad siRNA designated Bad siRNA-I and Bad siRNA-II as described in Materials and Methods. Both were able to significantly reduce Bad protein expression, whereas control siRNA had no significant effect (Fig. 8A and C). Depletion of Bad in Jurkat cells was found to significantly inhibit THC-mediated apoptosis when compared with Jurkat cells transfected with control siRNA (Fig. 8B and D). These data therefore corroborated our earlier results showing the crucial role of Bad in THC-mediated downstream signaling in induction of apoptosis of Jurkat cells.

Discussion

Recently, cannabinoids were shown to inhibit the proliferation of several human cancer cell lines, including leukemia (5, 10), breast (19), prostate (20), and gliomas (16). Studies from our laboratory showed that activation of cannabinoid receptors on normal and transformed T cells triggers apoptosis (10, 21). The data presented in the current study provide new insights into the functional roles of cannabinoid receptors and MAPK cascades in cannabinoid-mediated mitochondrial injury, caspase activation, and cell death. MAPK pathways consist of three parallel serine/threonine kinase (ERK, JNK, and the p38 MAPK) modules involved in the regulation of diverse cellular events, including proliferation, differentiation, apoptosis, etc. (22). In the current study, we investigated the effect of THC treatment on all three modules of MAPK signaling pathways in Jurkat cells and noted that THC-mediated cell death was associated with interruption of the Raf-1/MEK/ERK signaling
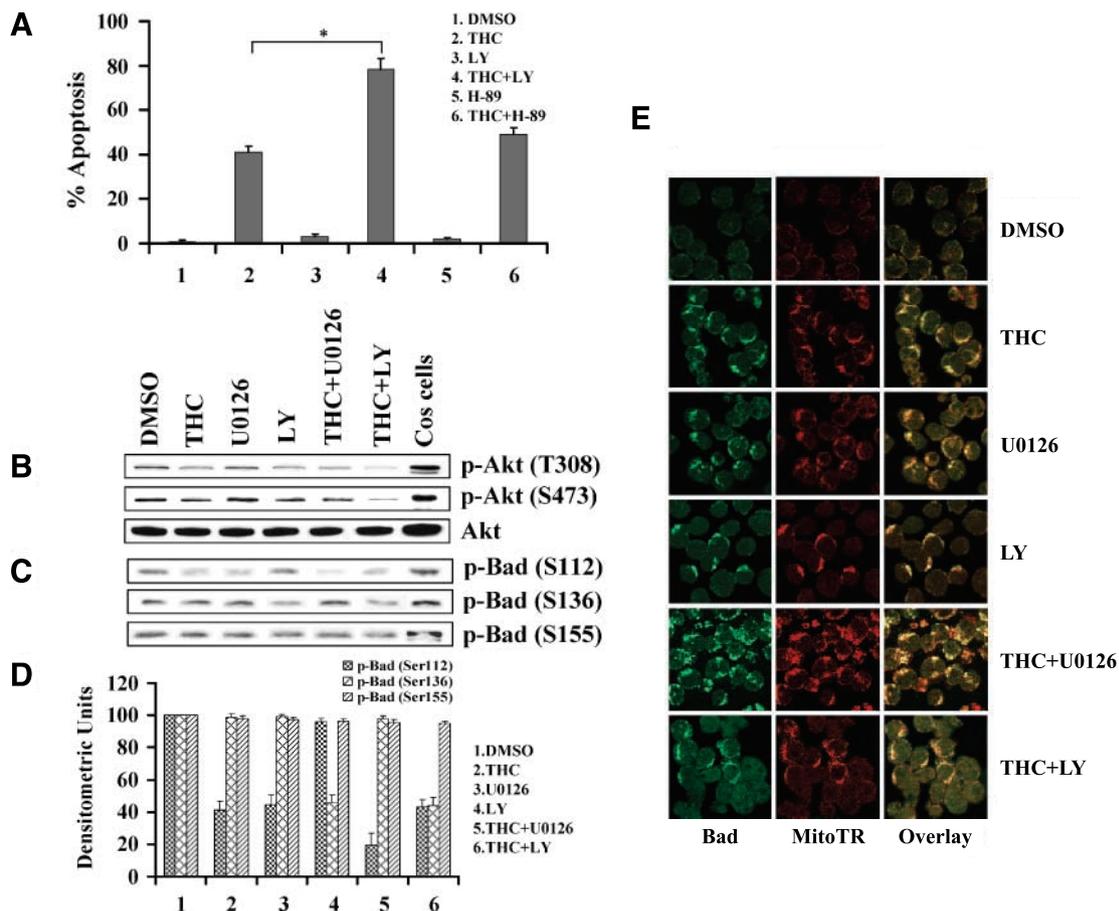

FIGURE 5. THC-induced apoptosis is blocked by PTX. **A.** Log-phase Jurkat cells were pretreated with either 50 or 100 ng/mL PTX for 16 hours in the presence or absence of 10 μmol/L THC for an additional 12 hours. The extent of apoptosis was determined as described in Fig. 1A. Columns, mean of three separate experiments done in triplicate; bars, SD. **B.** Cells were cultured with 50 ng/mL PTX for 16 hours in the presence or absence of 10 μmol/L THC for an additional 12 hours followed by immunoblotting of whole-cell lysates with antibodies that recognize phospho-Raf-1, Raf-1, phospho-MEK1/2, MEK1/2, phospho-ERK1/2, ERK1/2, phospho-RSK (Thr^{359}/Ser^{363}), RSK, phospho-p38, p38, phospho-JNK, and JNK. Levels of caspases and PARP were immunoassayed by culturing Jurkat cells with 50 ng/mL PTX for 16 hours in the presence or absence of 10 μmol/L THC for an additional 24 hours in medium containing 10% FBS. β-Actin served as a loading control. Representative of three independent experiments.

FIGURE 6. Effects of THC on mitochondrial localization of Bad in THC-stimulated cells. **A.** Jurkat cells were treated with either 15 μmol/L LY294002 (*LY*) or 2 μmol/L H-89 in medium containing 10% FBS in the absence or presence of 10 μmol/L THC for a total 12 hours, after which the percentage of apoptotic cells were determined as described in Fig. 1A. Columns, mean of three separate experiments done in triplicate; bars, SD. *, $P < 0.05$, significantly less than values obtained for the treated cells with THC + LY294002. **B.** Cells were cultured with either 15 μmol/L LY294002 or 25 μmol/L U0126 in medium containing 10% FBS in the absence or presence of 10 μmol/L THC for a total 12 hours, after which Western analysis was used to monitor expression of phospho-Akt (Thr[308]), phospho-Akt (Ser[473]), and Akt. Akt served as a loading control. **C.** Cells were cultured as described in **B**, after which precleared cell lysates were incubated overnight with mouse monoclonal anti-Bad IgG conjugated to protein A-agarose beads. Immunoprecipitates were subsequently subjected to Western analysis to monitor the phosphorylation status of phospho-Bad (Ser[112]), phospho-Bad (Ser[136]), and phospho-Bad (Ser[155]). All sites were analyzed on a single blot. Cos cells were used as a positive control. Representative experiment. Two additional studies yielded equivalent results. **D.** Quantitative changes in Bad phosphorylation were determined by densitometric analysis of immunoblots. Columns, mean of three independent experiments done in triplicate; bars, SD. **E.** Jurkat cells treated as described in **B**, after which cells were adhered to slides by cytospin and subjected to double staining with anti-Bad antibodies and Cy2-labeled secondary antibodies (*green*) followed by a mitochondrion-specific dye (MitoTracker Deep Red 633) and then analyzed by confocal microscopy. Similar results were obtained in three independent experiments.

pathway without significantly altering the p38 and JNK modules. Consequently, we further investigated the effect of THC on the upstream and downstream events that modulate the ERK module of MAPK. The pronounced down-regulation of phospho-Raf-1 was also associated with a marked reduction in phosphorylation of MEK, a major Raf-1 substrate (23), phospho-ERK, the primary MEK target (24), and RSK, the first substrate of ERK (25). This process occurred early, was dependent on cannabinoid receptor ligation, and proceeded upstream of caspase activation. THC also decreased the phosphorylation of Akt. However, no significant association of Bad translocation with PI3K/Akt and PKA signaling pathways was noted.

The regulation of mitochondrial membrane function and the release of apoptotic regulatory factors from mitochondria are key components of the apoptotic repertoire, tightly controlled by the Bcl-2 family proteins (26, 27). There is accumulated

evidence suggesting that the MAPK pathway, through Bad phosphorylation, plays a significant functional role in cell survival (26). The family of RSK was among the first cytoplasmic MAPK substrates identified (28). RSK phosphorylate a variety of substrates and regulate a diverse array of cellular functions, such as gene transcription, protein synthesis, and cell cycle regulation (29). Thus, MAPK activates RSK, which in turn catalyzes the phosphorylation of Bad (26). Cell survival is associated with the phosphorylation of Bad, which, by interacting with the scaffold protein 14-3-3 in the cytosol, prevents its translocation to the mitochondria (30). In the absence of survival signals, Bad is dephosphorylated, translocates to the mitochondria, and interacts with Bcl-2 and Bcl-X$_L$, thereby preventing the survival function of Bcl-2 and Bcl-X$_L$ (30, 31). Data from the present study showed that THC inactivated the cytoprotective serine/threonine kinase pathway

(Raf-1/MEK/ERK/RSK) that plays an important functional role in mediating Bad translocation. This may have caused the localization of Bad to the mitochondria as seen following THC treatment.

Based on these results, the effect of THC treatment on the PI3K/AKT and PKA signaling pathways was also examined in the regulation of Bad and cell death (32-34). Our findings indicated that THC caused the marked reduction in the level of phospho-Bad on site Ser[112] without significantly altering the PKA module. The effect on Bad Ser[112] was more pronounced when cells were exposed to THC in combination with U0126 consistent with recent studies that the MAPK-activated RSK phosphorylates Bad on Ser[112] (30, 35). Although there is down-regulation of phospho-AKT on both sites Thr[308] and Ser[473] following exposure of Jurkat cells to THC, no change was detected in phospho-Bad on the site Ser[136], which was reported to be implicated in this pathway (32, 33). This finding was confirmed by THC dose response and time course analysis when treated cells were examined in phosphorylation status of Bad on this site. Moreover, confocal analysis indicated that LY294002, an inhibitor of PI3K, failed to enhance the degree of Bad translocation following exposure of Jurkat cells to THC. In view of evidence linking the dysregulation of the PI3K/Akt progression to apoptosis, it is tempting to invoke this mechanism to explain the ability of THC and LY294002 to induce cell death in Jurkat cells. However, identification of the specific events responsible for PI3K inhibitor-mediated lethality remains an elusive goal. Akt is implicated in post-translational modification of Bad (32), regulation of the expression of antiapoptotic proteins, including Bcl-2 and XIAPS (36), and modulation of diverse pathways governing cell survival decisions, including those associated with GSK (37), mammalian target of rapamycin (38), nuclear factor-κB (39), etc. (40-42). In this regard, the finding that LY294002, an inhibitor of PI3K, failed to enhance THC-mediated translocation of Bad to mitochondria argues against a critical role for this pathway in regulation of Bad phosphorylation.

It has long been known that cannabinoids, including THC, can stimulate the MAPK cascade in Chinese hamster ovary cells (13), rat and mouse hippocampus (14), rat primary astrocytes (43), human astrocytoma cells (44), transformed neural cells (16, 45) human breast cancer cells (19), and the striatum (46). Furthermore, a recent report has shown evidence indicating that THC-induced apoptosis in certain types of leukemic cells is mediated by down-regulation of ERK (5). Our findings represented THC-mediated ERK inactivation and cell death in a variety of human tumor cell lines, which are consistent with this report in the literature (5). However, the precise role of cannabinoid receptor as a modulator of the ERK cascade is still a matter of debate. It is generally accepted that the activation of the ERK cascade leads to cell proliferation (47). However, recent investigations have begun to define situations in which ERK mediates cell cycle arrest (48), antiproliferation (49), and apoptotic (50) or nonapoptotic (51) death in many cell lines. In most but not all systems studied,


FIGURE 7. Enforced expression of constitutively active MEK blocks THC translocation of Bad to the mitochondria. **A.** Jurkat cells expressing constitutively active MEK (Mek/30) were exposed to U0126 (25 μmol/L) and THC (10 μmol/L) alone or in combination for 12 hours, after which proteins (prepared from cells in the absence and presence of doxycycline) were loaded onto the same SDS-PAGE followed by transferring onto a single piece of nitrocellulose, and the immunoprecipitates were subjected to Western analysis to monitor the phosphorylation status of phospho-Bad (Ser[112]), phospho-Bad (Ser[136]), and phospho-Bad (Ser[155]) at same incubation time. Representative experiment. Two additional studies yielded equivalent results. **B.** Cell lysates were prepared from clones (Mek/30) of Jurkat cells as described in **A**, after which cells were adhered to slides by cytospin and subjected to double staining with anti-Bad antibodies and Cy2-labeled secondary antibodies (green) followed by a mitochondrion-specific dye (MitoTracker Deep Red 633) and then analyzed by confocal microscopy. Representative of three independent experiments.
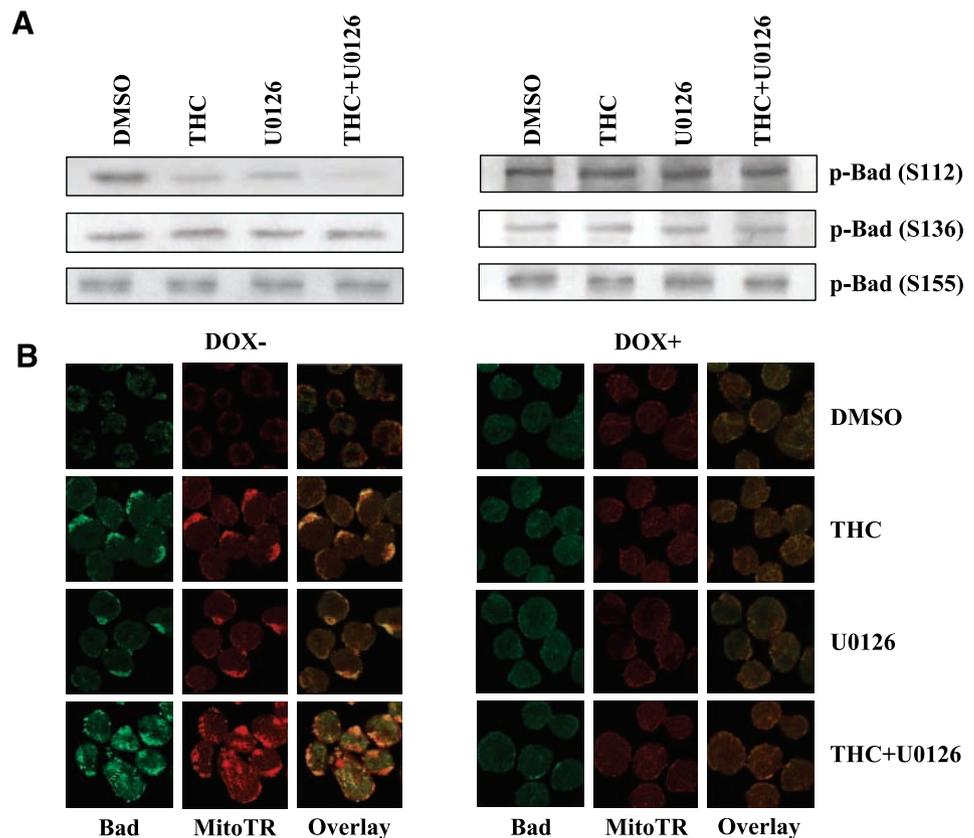
inactivation of MEK and ERK is associated with the promotion of cell death (52, 53). The mechanism by which this occurs is not known with certainty but may vary based on the cell type. Except this, it may be related to perturbations in downstream ERK targets, including the Elk (54), CREB family of transcription factors (35), etc. Alternatively, inactivation of ERK may prevent phosphorylation of Bad and in so doing preserve its proapoptotic capacity through interaction with Bcl-2/Bcl-X$_L$ (26, 27). To further define the functional role of the MEK/ERK/RSK pathway in the translocation of Bad to mitochondria, Jurkat cells that were stably transfected with a constitutively active MEK construct were employed. Consistent with this model, enforced expression of constitutively active MEK overcame the suppression of ERK/RSK activation and the reduction in the levels of phospho-Bad on Ser^{112} and

substantially protected cells from THC/U0126 lethality. In fact, the protection effects of enforced ERK activation plays an important role in blocking the localization of Bad to mitochondria. However, given the pleiotropic nature of THC action, the possibility that other downstream targets of this agent contribute to lethality cannot be excluded. The relation between activation of the ERK cascade and cell proliferation/antiproliferation depends on various stimuli (55) and varies between diverse types of cells (56, 57).

In a recent study, it was shown that C6 glioma cells exposed to a synthetic cannabinoid, WIN 55,212-2, exhibited down-regulation of the Akt and ERK signaling pathways before induction of apoptosis (58). Exposure to WIN 55,212-2 caused a decrease in phospho-Bad. In addition, Powles et al. (5) showed that THC-induced cell death in leukemic cells was
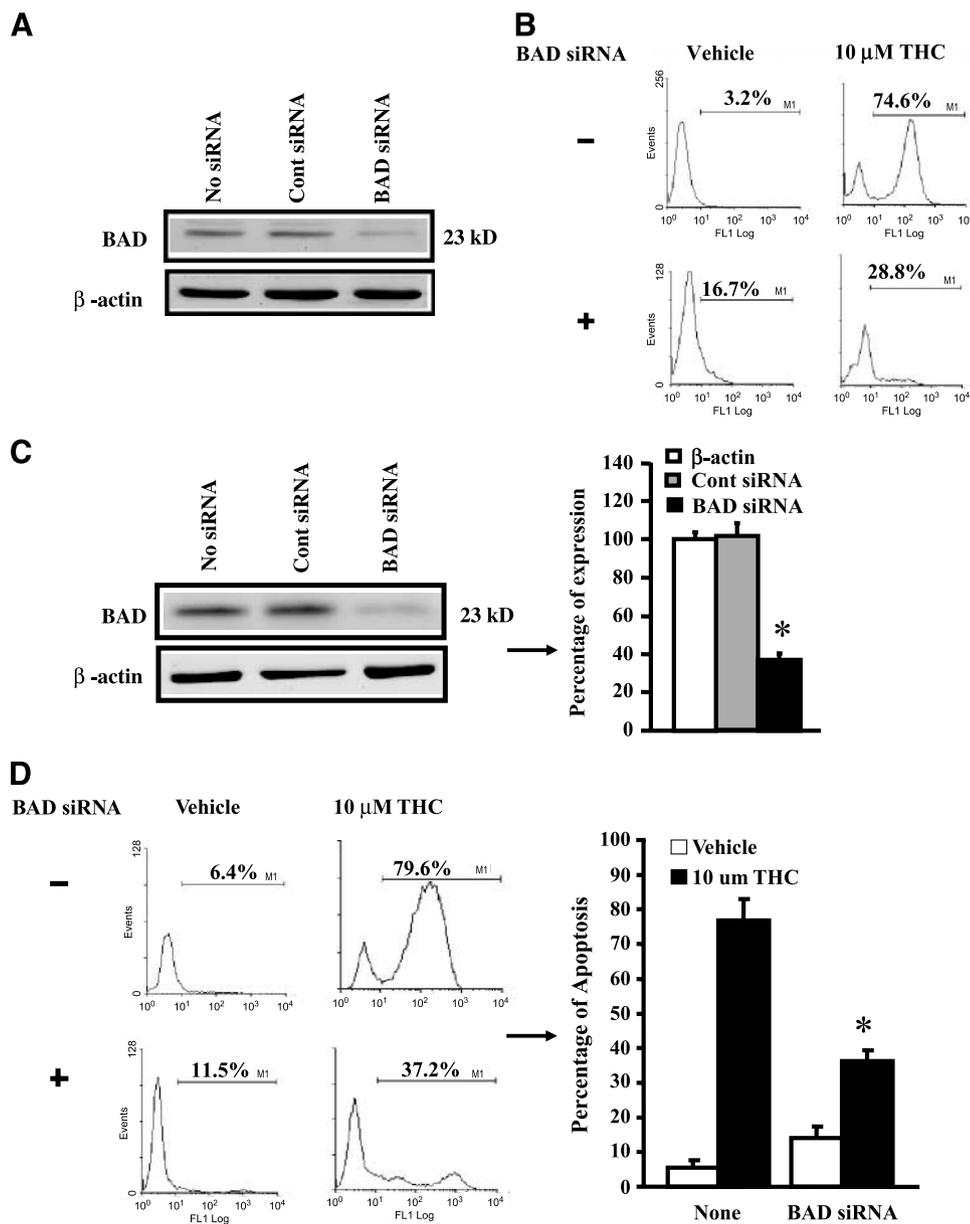
FIGURE 8. Bad plays a critical role in THC-induced apoptosis. **A** and **B.** Jurkat cells were transfected with Bad siRNA-I. **C** and **D.** Cells were transfected with siRNA-II as described in Materials and Methods. **A** and **C.** Bad expression level was analyzed by Western blotting using antibody against Bad. **B** and **D.** Jurkat cells transfected with Bad siRNA were cultured with vehicle or THC and analyzed for apoptosis using TUNEL assay. **C.** Right, signal intensity when compared with β-actin. Columns, mean of three independent experiments; bars, SE. **D.** Right, percent apoptosis. Columns, mean of three independent experiments; bars, SE. *, $P < 0.05$, compared with controls.

preceded by significant changes in the expression of genes involved in MAPK signal transduction pathways. The current study further extends these observation in a leukemia model by identifying Raf-1/MEK/ERK/RSK-mediated localization of Bad to mitochondria as a critical mechanism regulating cannabinoid-induced lethality. This was supported by the observation that enforced expression of constitutively active MEK/ERK resulted in the inhibition of mitochondrial Bad localization, caspase activation, and apoptosis. Moreover, down-regulation of Bad expression by siRNA led to marked resistance of Jurkat cells to THC-mediated apoptosis. Although the ERK pathway has been shown to play a pivotal role in regulating cell growth and differentiation to growth factors, cytokines, and phorbol esters (59), it is also weakly activated by stress (60, 61). In contrast, JNK and p38 are weakly activated by growth factors but are highly activated in response to stress signals, including tumor necrosis factor, ionizing and UV irradiation, and hyperosmotic stress, which lead to induction of apoptosis (53, 62). For example, there is mixed evidence for the role of ERK in influencing cell survival of cisplatin-treated cells. Some studies have suggested that ERK activation is associated with enhanced survival of cisplatin-treated cells (63, 64), whereas others have shown that elevated expression of Ras, an upstream component of the ERK signaling pathway, leads to increased sensitivity to the drug (65).

THC and other cannabinoids can induce apoptosis in a variety of tumor cell lines, thereby raising the possibility of the use of cannabinoids as novel anticancer agents (11). However, the use of cannabinoids that activate CB1 receptors is severely limited by their psychoactive effects. The fact that malignant cells of the immune system express CB2 receptors that can be targeted to induce apoptosis offers a novel approach to use CB2 select agonists as anticancer drugs with no psychoactive properties. Because CB2 receptors are almost exclusively expressed on immune cells, the use of CB2 select agonists should not exert generalized toxicity that is common to other modes of treatment, such as radiation or chemotherapy. One possible drawback could be that use of select CB2 agonists to kill tumor cells may also cause immunosuppression. Thus, further studies are necessary to address the relative sensitivity of normal and transformed immune cells to CB2 agonists *in vivo*. Identifying the molecular pathways that trigger apoptosis following ligation of cannabinoid receptors is critical in understanding how endogenous and exogenous cannabinoids may regulate the growth of normal and transformed immune cells. The current study provides useful and novel information on developing a new class of anticancer drugs by targeting cannabinoid CB2 receptors.

Materials and Methods
Cells
Jurkat, Molt4, SupT1, Hut78, and U251 glioma cell lines were purchased from American Type Culture Collection (Rockville, MD). The cells were cultured in RPMI 1640 supplemented with 10% fetal bovine serum (FBS; Atlanta, Norcross, GA). They were maintained in a 37°C, 5% CO_2, fully humidified incubator.

Reagents
THC was obtained from the National Institute of Drug Abuse (Rockville, MD). SR141716 and SR144528 were obtained from Sanofi Recherche (Montpellier, France). PTX and LY294002 were purchased from Sigma (St. Louis, MO). 3,3-Dihexyloxacarbocyanine iodide, U0126, PMA, and the PKA inhibitor H-89 were purchased from Calbiochem (San Diego, CA). Annexin V/PI was purchased from BD PharMingen (San Diego, CA). The pan-caspase inhibitor Z-VAD-FMK was purchased from R&D Systems (Minneapolis, MN) and all agents were initially dissolved in DMSO (Sigma) as stock solution and stored at −20°C.

Detection of THC-Induced Apoptosis In vitro
Jurkat cells (4×10^5 per well) were cultured in 24-well plates in the presence or absence of designated concentrations of THC for 12 to 24 hours. After cytospin, the cell preparations were stained with Wright-Giemsa and viewed by light microscopy to evaluate the extent of apoptosis as described previously (52). The percentage of apoptotic cells was determined by evaluating ≥500 cells per treatment in triplicate. To confirm the results of morphologic analysis, TUNEL method was used as described elsewhere (66).

Flow Cytometry to Detect Apoptosis by TUNEL
Following each treatment, the cells were harvested, washed twice with PBS, and fixed with 4% paraformaldehyde for 30 minutes at room temperature. The cells were then permeabilized on ice for 2 minutes, incubated with FITC-dUTP and terminal deoxynucleotidyl transferase (Boehringer Mannheim, Indianapolis, IN) for 1 hour at 37°C and 5% CO_2, and analyzed using a Beckman Coulter Cytomics FC 500 (Fullerton, CA).

Determination of MMP
MMP was monitored using 3,3-dihexyloxacarbocyanine iodide as described (9). For each condition, 4×10^5 cells were incubated in 1 mL 3,3-dihexyloxacarbocyanine iodide (40 nmol/L) at 37°C in for 15 minutes and subsequently analyzed using a Becton Dickinson FACScan cytofluorometer (Mansfield, MA) with excitation and emission settings of 488 and 525 nm, respectively. Control experiments documenting the loss of MMP were done by exposing cells to 5 μmol/L carbamoyl cyanide *m*-chlorophenylhydrazone (Sigma; 15 minutes, 37°C), an uncoupling agent that abolishes the MMP.

Annexin V/PI
Annexin V/PI staining was done as described previously (10). The cells were analyzed using a Becton Dickinson FACScan flow cytometer.

RNA Isolation and Reverse Transcription-PCR
RNA was isolated from $\sim 1 \times 10^7$ cells using the RNeasy Mini kit (Qiagen, Valencia, CA) according to the recommendations from the manufacturer. DNA was removed by the RNase-free DNase set (Qiagen) following RNA isolation. RNA concentration was determined spectrophotometrically, and the integrity of the each preparation was verified by agarose gel

electrophoresis. cDNA was synthesized by reverse transcription of 50 ng total RNA as template for first-strand synthesis using the Sensiscript RT kit (Qiagen). All PCR was prepared using MasterAmp PCR Premix F (Epicenter Technologies, Madison, WI) according to the recommendations from the manufacturer and using Platinum Taq DNA polymerase (Invitrogen, Carlsbad, CA). Human CB1 was amplified using primers HCB1U (5′-CG-TGGGCAGCCTGTTCCTCA-3′) and HCB1L (5′-CATGC-GGGCTTGGTCTGG-3′), which yield a product of 403 bp. Human CB2 was amplified using primers HCB2U (5′-CGCC-GGAAGCCCTCATACC-3′) and HCB2L (5′-CCTCATTCG-GGCCATTCCTG-3′), which yield a product of 522 bp. β-Actin was used as a positive control, with primers BAU (5′-AAGG-CCAACCGTGAAAAGATGACC-3′) and BAL (5′-ACCGCTC-GTTGCCAATAGTGATGA-3′), with a product size of 427 bp. PCR was carried out using the following variables: 95°C for 10 seconds, 59°C for 20 seconds, and 72°C for 45 seconds for 35 cycles followed by a final 1 minute at 72°C in an Applied Biosystems GeneAmp 9700 (Foster City, CA). The resulting PCR products were separated on a 1.2% agarose gel.

Immunoblot Analysis

Immunoblotting was done as described previously (52). The source of antibodies was as follows: caspase-2 (Alexis, San Diego, CA); Bid, phospho-ERK1/2 (Thr^{202}/Tyr^{204}), JNK, phospho-JNK, phospho-38, phospho-p38 MAPK, phospho-Akt (Thr^{308}), phospho-Akt (Ser^{473}), Akt, and Bad (C-7; Santa Cruz Biotechnology, Santa Cruz, CA); Bad, phospho-Bad (Ser^{112}), phospho-Bad (Ser^{136}), phospho-Bad (Ser^{155}), caspase-3, caspase-8, caspase-9, caspase-10, ERK1/2, PARP, MEK1/2, phospho-MEK1/2, p90RSK, phospho-p90RSK (Thr^{359}/Ser^{363}), phospho-p90RSK (Ser^{380}), and phospho-p90RSK (Thr^{573}; Cell Signaling Technology, Danvers, MA); c-Raf-1, phospho-c-Raf-1 (Biosource, Camarillo, CA); and β-actin (Sigma). Cell lysates were prepared and the concentration of the protein was measured by using standard Bradford assays. The proteins were fractionated in SDS-PAGE and transferred onto polyvinylidene difluoride membranes using a dry-blot apparatus (Bio-Rad, Hercules, CA). The membrane was incubated in blocking buffer for 1 hour at room temperature followed by incubation in primary antibody at 4°C overnight. The membrane was then washed thrice (10-15 minutes) with washing buffer (PBS-0.2% Tween 20) and incubated for 1 hour in horseradish peroxidase–conjugated secondary antibody (Cell Signaling Technology, Inc.) in blocking buffer. The membranes were then washed several times and incubated in developing solution (equal volume of solutions A and B; Enhanced Chemiluminescence Western Blotting Detection Reagents, Amersham Biosciences, Little Chalfont, United Kingdom) and signal was detected using ChemiDoc System (Bio-Rad). Densitometric analyses of the Western blots were done with UN-SCAN-IT (Silk Scientific, Orem, UT) software digitizer technology.

Immunoprecipitation

After drug treatments, cells were washed with PBS and incubated for 10 minutes in lysis buffer [150 mmol/L NaCl, 50 mmol/L Tris-HCl (pH 8.0), 1 mmol/L EDTA, 1% (v/v) NP40, 0.25% (w/v) sodium deoxycholate, 1 mmol/L NaF, 1 mmol/L sodium pyrophosphate, 100 μmol/L Na$_3$VO$_4$, 1 mmol/L

phenylmethylsulfonyl fluoride, 10 μg/mL aprotinin, 10 μg/mL leupeptin]. Precleared by incubation with protein A-agarose bead slurry, cell lysates (2 μg/μL total cell protein) were incubated overnight with mouse monoclonal anti-Bad IgG or rabbit polyclonal anti-Bad IgG conjugated to agarose beads. Immunoprecipitates were captured by addition of protein A-agarose. The agarose beads were collected by centrifugation, washed twice in ice-cold lysis buffer, boiled in Laemmli sample buffer, and subjected to SDS-PAGE and subsequent immunoblot analysis.

Tet-On-Inducible Jurkat Cell Lines

Stably transfected Jurkat clones that inducibly expressed constitutively active MEK1 were generated as described (52). To test for the induced expression of the hemagglutinin-tagged MEK1, stable clones were left untreated or were treated for designated periods with 2 μg/mL doxycycline (Sigma), harvested, and analyzed for expression of the appropriate protein by Western blot as described above.

Transfection of Jurkat Cells with Mouse Bad siRNA

Jurkat cells (5 × 10^6) were transfected with 1.7 μmol/L human siRNA (5′-GAAGGGACUUCCUCGCCCGTT-3′; 5′-CGGGCGAGGAAGUCCCUUCTT-3′; designated siRNA-I; Cell Signaling Technology, Inc., Danvers, MA) using nucleofection of Jurkat cells with Transfection Reagent kit and Nucleofactor II electroporation system following the protocols of the company (Amaxa, Inc., Gaithersburg, MD). Jurkat cells were also transfected with human-specific control siRNA (1.7 μmol/L) conjugated with fluorescein (Cell Signaling Technology, Inc., Danvers, MA) and pmaxGFP plasmid (2 μg; Amaxa). In a separate experiment, 5 × 10^6 Jurkat cells were also transfected with human Bad siRNA (siGENOME SMARTpool reagent M-003870-02; 3 μg; Dharmacon RNA Technologies, Lafayette, CO; designated siRNA-II) using nucleofection of Jurkat cells with Transfection Reagent kit and Nucleofactor II electroporation system following the protocols of the company. As a control, 5 × 10^6 Jurkat cells were transfected with human-specific negative control SiGLO RISK-free siRNA (3 μg; designated control siRNA-II) unconjugated or conjugated with Cy-3 (Pool D-001206-13-05; Dharmacon RNA Technologies) and pmaxGFP plasmid (2 μg). Transfected Jurkat cells were cultured for 48 hours in complete medium at 37°C and 5% CO$_2$. We observed >90% cell viability after transfection. To examine the efficiency of transfection, we observed pmaxGFP plasmid-transfected Jurkat cells under fluorescent microscope and observed >50% cells expressing green fluorescent protein. We also examined the expression of green fluorescent protein by performing flow cytometry. Jurkat cells, untransfected or transfected with control siRNA or human Bad siRNA, were treated with vehicle or THC, and 24 hours after treatment, cells were harvested and apoptosis was determined by performing TUNEL assay and using flow cytometry.

Immune Complex Kinase Assay (a Nonradioactive Method)

ERK activity was measured in THC-treated cell lysates using p44/42 MAPK Assay kit (Cell Signaling Technology, Inc., Danvers, MA).

DNA Fragmentation Assay

For qualitative assessment of internucleosomal DNA fragmentation, DNA was extracted from cell lysates after the appropriate treatment and subjected to agarose gel electrophoresis as described previously (67).

Confocal Microscopy

Confocal microscope images were captured on a LSM 510 microscope with a ×60, 1.3 NA Apochromat objective (Carl Zeiss, Inc., Thornwood, NY). Jurkat cells were grown as described above on a 24-well plate (Corning, Corning, NY). After treatment, confocal microscopy of cells was done after double staining with primary antibody against Bad and mitochondrion-specific dye (MitoTracker Deep Red 633; Molecular Probes, Inc. Eugene, OR) as indicated in individual experiments. The excitation wavelength for Bad and Mito-Tracker Deep Red 633 were 490 and 644 nm, respectively.

Statistical Analysis

The significance of differences between experimental conditions was determined using the two-tailed Student's *t* test. To characterize synergistic or antagonistic interactions between agents, median dose effect analysis (68) was employed using a commercially available software program (Calcusyn, Biosoft, Ferguson, MO).

References

1. Watson SJ, Benson JA, Jr., Joy JE. Marijuana and medicine: assessing the science base: a summary of the 1999 Institute of Medicine report. Arch Gen Psychiatry 2000;57:547–52.

2. Matsuda LA, Lolait SJ, Brownstein MJ, Young AC, Bonner TI. Structure of a cannabinoid receptor and functional expression of the cloned cDNA. Nature 1990;346:561–4.

3. Munro S, Thomas KL, Abu-Shaar M. Molecular characterization of a peripheral receptor for cannabinoids. Nature 1993;365:61–5.

4. Pertwee RG. Pharmacology of cannabinoid CB1 and CB2 receptors. Pharmacol Ther 1997;74:129–80.

5. Powles T, te Poele R, Shamash J, et al. Cannabis-induced cytotoxicity in leukemic cell lines: the role of the cannabinoid receptors and the MAPK pathway. Blood 2005;105:1214–21.

6. Vincent BJ, McQuiston DJ, Einhorn LH, Nagy CM, Brames MJ. Review of cannabinoids and their antiemetic effectiveness. Drugs 1983;25 Suppl 1:52–62.

7. Roth MD, Baldwin GC, Tashkin DP. Effects of Δ-9-tetrahydrocannabinol on human immune function and host defense. Chem Phys Lipids 2002;121:229–39.

8. Do Y, McKallip RJ, Nagarkatti M, Nagarkatti PS. Activation through cannabinoid receptors 1 and 2 on dendritic cells triggers NF-κB-dependent apoptosis: novel role for endogenous and exogenous cannabinoids in immunoregulation. J Immunol 2004;173:2373–82.

9. Lombard C, Nagarkatti M, Nagarkatti SP. Targeting cannabinoid receptors to treat leukemia: role of cross-talk between extrinsic and intrinsic pathways in Δ(9)-tetrahydrocannabinol (THC)-induced apoptosis of Jurkat cells. Leuk Res 2005;29: 915–22.

10. McKallip RJ, Lombard C, Fisher M, et al. Targeting CB2 cannabinoid receptors as a novel therapy to treat malignant lymphoblastic disease. Blood 2002; 100:627–34.

11. Guzman M. Cannabinoids: potential anticancer agents. Nat Rev Cancer 2003; 3:745–55.

12. Bouaboula M, Poinot-Chazel C, Bourrie B, et al. Activation of mitogen-activated protein kinases by stimulation of the central cannabinoid receptor CB1. Biochem J 1995;312:637–41.

13. Rueda D, Galve-Roperh I, Haro A, Guzman M. The CB(1) cannabinoid receptor is coupled to the activation of c-Jun N-terminal kinase. Mol Pharmacol 2000;58:814–20.

14. Derkinderen P, Ledent C, Parmentier M, Girault JA. Cannabinoids activate p38 mitogen-activated protein kinases through CB1 receptors in hippocampus. J Neurochem 2001;77:957–60.

15. Rueda D, Navarro B, Martinez-Serrano A, Guzman M, Galve-Roperh I. The endocannabinoid anandamide inhibits neuronal progenitor cell differentiation through attenuation of the Rap1/B-Raf/ERK pathway. J Biol Chem 2002;277: 46645–50.

16. Galve-Roperh I, Sanchez C, Cortes ML, del Pulgar TG, Izquierdo M, Guzman M. Anti-tumoral action of cannabinoids: involvement of sustained ceramide accumulation and extracellular signal-regulated kinase activation. Nat Med 2000;6:313–9.

17. Gomez Del Pulgar T, De Ceballos ML, Guzman M, Velasco G. Cannabinoids protect astrocytes from ceramide-induced apoptosis through the phosphatidylinositol 3-kinase/protein kinase B pathway. J Biol Chem 2002;277:36527–33.

18. Eisenmann KM, VanBrocklin MW, Staffend NA, Kitchen SM, Koo HM. Mitogen-activated protein kinase pathway-dependent tumor-specific survival signaling in melanoma cells through inactivation of the proapoptotic protein bad. Cancer Res 2003;63:8330–7.

19. Melck D, Rueda D, Galve-Roperh I, De Petrocellis L, Guzman M, Di Marzo V. Involvement of the cAMP/protein kinase A pathway and of mitogen-activated protein kinase in the anti-proliferative effects of anandamide in human breast cancer cells. FEBS Lett 1999;463:235–40.

20. Ruiz L, Miguel A, Diaz-Laviada I. Δ9-Tetrahydrocannabinol induces apoptosis in human prostate PC-3 cells via a receptor-independent mechanism. FEBS Lett 1999;458:400–4.

21. McKallip RJ, Lombard C, Martin BR, Nagarkatti M, Nagarkatti PS. Δ(9)-Tetrahydrocannabinol-induced apoptosis in the thymus and spleen as a mechanism of immunosuppression *in vitro* and *in vivo*. J Pharmacol Exp Ther 2002;302:451–65.

22. Chang L, Karin M. Mammalian MAP kinase signalling cascades. Nature 2001;410:37–40.

23. Hipskind RA, Baccarini M, Nordheim A. Transient activation of RAF-1, MEK, ERK2 coincides kinetically with ternary complex factor phosphorylation and immediate-early gene promoter activity *in vivo*. Mol Cell Biol 1994;14: 6219–31.

24. Troppmair J, Bruder JT, Munoz H, et al. Mitogen-activated protein kinase/extracellular signal-regulated protein kinase activation by oncogenes, serum, and 12-*O*-tetradecanoylphorbol-13-acetate requires Raf and is necessary for transformation. J Biol Chem 1994;269:7030–5.

25. Smith JA, Poteet-Smith CE, Malarkey K, Sturgill TW. Identification of an extracellular signal-regulated kinase (ERK) docking site in ribosomal S6 kinase, a sequence critical for activation by ERK *in vivo*. J Biol Chem 1999;274:2893–8.

26. Korsmeyer SJ. BCL-2 gene family and the regulation of programmed cell death. Cancer Res 1999;59:1693–700s.

27. Kroemer G, Reed JC. Mitochondrial control of cell death. Nat Med 2000;6: 513–9.

28. Frodin M, Gammeltoft S. Role and regulation of 90 kDa ribosomal S6 kinase (RSK) in signal transduction. Mol Cell Endocrinol 1999;151:65–77.

29. Gavin AC, Ni Ainle A, Chierici E, Jones M, Nebreda AR. A p90(rsk) mutant constitutively interacting with MAP kinase uncouples MAP kinase from p34(cdc2)/cyclin B activation in *Xenopus* oocytes. Mol Biol Cell 1999;10: 2971–86.

30. Zha J, Harada H, Yang E, Jockel J, Korsmeyer SJ. Serine phosphorylation of death agonist BAD in response to survival factor results in binding to 14-3-3 not BCL-X(L). Cell 1996;87:619–28.

31. Scheid MP, Duronio V. Dissociation of cytokine-induced phosphorylation of Bad and activation of PKB/Akt: involvement of MEK upstream of Bad phosphorylation. Proc Natl Acad Sci U S A 1998;95:7439–44.

32. Datta SR, Dudek H, Tao X, et al. Akt phosphorylation of BAD couples survival signals to the cell-intrinsic death machinery. Cell 1997;91:231–41.

33. del Peso L, Gonzalez-Garcia M, Page C, Herrera R, Nunez G. Interleukin-3-induced phosphorylation of BAD through the protein kinase Akt. Science 1997; 278:687–9.

34. Zhou XM, Liu Y, Payne G, Lutz RJ, Chittenden T. Growth factors inactivate the cell death promoter BAD by phosphorylation of its BH3 domain on Ser[155]. J Biol Chem 2000;275:25046–51.

35. Bonni A, Brunet A, West AE, Datta SR, Takasu MA, Greenberg ME. Cell survival promoted by the Ras-MAPK signaling pathway by transcription-dependent and -independent mechanisms. Science 1999;286:1358–62.

36. Leverrier Y, Thomas J, Mathieu AL, Low W, Blanquier B, Marvel J. Role of PI3-kinase in Bcl-X induction and apoptosis inhibition mediated by IL-3 or IGF-1 in Baf-3 cells. Cell Death Differ 1999;6:290–6.

37. Pap M, Cooper GM. Role of glycogen synthase kinase-3 in the

phosphatidylinositol 3-kinase/Akt cell survival pathway. J Biol Chem 1998;273: 19929 – 32.

38. Edinger AL, Thompson CB. Akt maintains cell size and survival by increasing mTOR-dependent nutrient uptake. Mol Biol Cell 2002;13:2276 – 88.

39. Gelfanov VM, Burgess GS, Litz-Jackson S, et al. Transformation of interleukin-3-dependent cells without participation of Stat5/bcl-xL: cooperation of Akt with Raf/Erk leads to p65 nuclear factor κB-mediated antiapoptosis involving c-IAP2. Blood 2001;98:2508 – 17.

40. Vanhaesebroeck B, Waterfield MD. Signaling by distinct classes of phosphoinositide 3-kinases. Exp Cell Res 1999;253:239 – 54.

41. Vanhaesebroeck B, Alessi DR. The PI3K-PDK1 connection: more than just a road to PKB. Biochem J 2000;346:561 – 76.

42. Nicholson KM, Anderson NG. The protein kinase B/Akt signalling pathway in human malignancy. Cell Signal 2002;14:381 – 95.

43. Sanchez C, Galve-Roperh I, Rueda D, Guzman M. Involvement of sphingomyelin hydrolysis and the mitogen-activated protein kinase cascade in the Δ9-tetrahydrocannabinol-induced stimulation of glucose metabolism in primary astrocytes. Mol Pharmacol 1998;54:834 – 43.

44. Bouaboula M, Bourrie B, Rinaldi-Carmona M, Shire D, Le Fur G, Casellas P. Stimulation of cannabinoid receptor CB1 induces krox-24 expression in human astrocytoma cells. J Biol Chem 1995;270:13973 – 80.

45. Sanchez C, Galve-Roperh I, Canova C, Brachet P, Guzman M. Δ9-Tetrahydrocannabinol induces apoptosis in C6 glioma cells. FEBS Lett 1998;436: 6 – 10.

46. Valjent E, Pages C, Rogard M, Besson MJ, Maldonado R, Caboche J. Δ9-Tetrahydrocannabinol-induced MAPK/ERK and Elk-1 activation *in vivo* depends on dopaminergic transmission. Eur J Neurosci 2001;14:342 – 52.

47. Derkinderen P, Enslen H, Girault JA. The ERK/MAP-kinases cascade in the nervous system. Neuroreport 1999;10:R24 – 34.

48. Pumiglia KM, Decker SJ. Cell cycle arrest mediated by the MEK/mitogen-activated protein kinase pathway. Proc Natl Acad Sci U S A 1997;94:448 – 52.

49. York RD, Yao H, Dillon T, et al. Rap1 mediates sustained MAP kinase activation induced by nerve growth factor. Nature 1998;392:622 – 6.

50. Mohr S, McCormick TS, Lapetina EG. Macrophages resistant to endogenously generated nitric oxide-mediated apoptosis are hypersensitive to exogenously added nitric oxide donors: dichotomous apoptotic response independent of caspase 3 and reversal by the mitogen-activated protein kinase kinase (MEK) inhibitor PD 098059. Proc Natl Acad Sci U S A 1998;95: 5045 – 50.

51. Murray B, Alessandrini A, Cole AJ, Yee AG, Furshpan EJ. Inhibition of the p44/42 MAP kinase pathway protects hippocampal neurons in a cell-culture model of seizure activity. Proc Natl Acad Sci U S A 1998;95: 11975 – 80.

52. Jia W, Yu C, Rahmani M, et al. Synergistic antileukemic interactions between 17-AAG and UCN-01 involve interruption of RAF/MEK- and AKT-related pathways. Blood 2003;102:1824 – 32.

53. Xia Z, Dickens M, Raingeaud J, Davis RJ, Greenberg ME. Opposing effects of ERK and JNK-p38 MAP kinases on apoptosis. Science 1995;270:1326 – 31.

54. Gille H, Kortenjann M, Thomae O, et al. ERK phosphorylation potentiates Elk-1-mediated ternary complex formation and transactivation. EMBO J 1995;14: 951 – 62.

55. Marshall CJ. Signal transduction. Taking the Rap. Nature 1998;392:553 – 4.

56. Johnson GL, Lapadat R. Mitogen-activated protein kinase pathways mediated by ERK, JNK, p38 protein kinases. Science 2002;298:1911 – 2.

57. Howe AK, Aplin AE, Juliano RL. Anchorage-dependent ERK signaling—mechanisms and consequences. Curr Opin Genet Dev 2002;12:30 – 5.

58. Ellert-Miklaszewska A, Kaminska B, Konarska L. Cannabinoids down-regulate PI3K/Akt and Erk signalling pathways and activate proapoptotic function of Bad protein. Cell Signal 2005;17:25 – 37.

59. Robinson MJ, Cobb MH. Mitogen-activated protein kinase pathways. Curr Opin Cell Biol 1997;9:180 – 6.

60. Guyton KZ, Liu Y, Gorospe M, Xu Q, Holbrook NJ. Activation of mitogen-activated protein kinase by H_2O_2. Role in cell survival following oxidant injury. J Biol Chem 1996;271:4138 – 42.

61. Aikawa R, Komuro I, Yamazaki T, et al. Oxidative stress activates extracellular signal-regulated kinases through Src and Ras in cultured cardiac myocytes of neonatal rats. J Clin Invest 1997;100:1813 – 21.

62. Chen YR, Wang X, Templeton D, Davis RJ, Tan TH. The role of c-Jun N-terminal kinase (JNK) in apoptosis induced by ultraviolet C and γ radiation duration of JNK activation may determine cell death and proliferation. J Biol Chem 1996;271:31929 – 36.

63. Hayakawa J, Ohmichi M, Kurachi H, et al. Inhibition of extracellular signal-regulated protein kinase or c-Jun N-terminal protein kinase cascade, differentially activated by cisplatin, sensitizes human ovarian cancer cell line. J Biol Chem 1999;274:31648 – 54.

64. Persons DL, Yazlovitskaya EM, Cui W, Pelling JC. Cisplatin-induced activation of mitogen-activated protein kinases in ovarian carcinoma cells: inhibition of extracellular signal-regulated kinase activity increases sensitivity to cisplatin. Clin Cancer Res 1999;5:1007 – 14.

65. Fokstuen T, Rabo YB, Zhou JN, et al. The Ras farnesylation inhibitor BZA-5B increases the resistance to cisplatin in a human melanoma cell line. Anticancer Res 1997;17:2347 – 52.

66. Chen D, McKallip RJ, Zeytun A, et al. CD44-deficient mice exhibit enhanced hepatitis after concanavalin A injection: evidence for involvement of CD44 in activation-induced cell death. J Immunol 2001;166:5889 – 97.

67. Jarvis WD, Povirk LF, Turner AJ, et al. Effects of bryostatin 1 and other pharmacological activators of protein kinase C on 1-[β-D-arabinofuranosyl]cyto-sine-induced apoptosis in HL-60 human promyelocytic leukemia cells. Biochem Pharmacol 1994;47:839 – 52.

68. Chou TC, Talalay P. Quantitative analysis of dose-effect relationships: the combined effects of multiple drugs or enzyme inhibitors. Adv Enzyme Regul 1984;22:27 – 55.